Structural Safety 56 (2015) 39–51

Contents lists available at ScienceDirect

Structural Safety

journal homepage: www.elsevier.com/locate/strusafe

Multi-variate seismic demand modelling using copulas: Application to non-ductile reinforced concrete frame in Victoria, Canada

Katsuichiro Goda [a,*], Solomon Tesfamariam [b]

[a] Department of Civil Engineering, University of Bristol, United Kingdom
[b] School of Engineering, University of British Columbia, Canada

ARTICLE INFO

Article history:
Received 26 July 2014
Received in revised form 20 May 2015
Accepted 21 May 2015

Keywords:
Seismic demand
Peak drift
Residual drift
Copula
Non-ductile RC frame

ABSTRACT

Joint probabilistic characteristics of key structural demand variables due to intense ground shaking are important for quantitative seismic loss estimation. Current damage–loss models require inputs of multiple seismic demand parameters, such as maximum/residual inter-storey drift ratio (ISDR) and peak floor acceleration (PFA). This study extends current seismic demand estimation methods based on incremental dynamic analysis (IDA) by characterising dependence among different engineering demand parameters (EDP) using copulas explicitly. The developed method is applied to a 4-storey non-ductile reinforced concrete (RC) frame in Victoria, British Columbia, Canada. The developed multi-variate seismic demand model is integrated with a storey-based damage–loss model to assess the economic consequences due to different earthquake loss generation modes (i.e. non-collapse repairs, collapse, and demolition). Results obtained from this study indicate that the effects of multi-variate seismic demand modelling on the expected seismic loss ratios are significant. The critical information is the limit state threshold for demolition. In addition, consideration of a realistic dependence structure of maximum and residual inter-storey drift ratios can be important for seismic loss estimation as well as for multi-criteria seismic performance evaluation.

1. Introduction

An accurate assessment of potential impact of future destructive earthquakes is essential for effective disaster risk reduction. Probabilistic seismic risk analysis (PSRA) entails the state-of-the-art understanding of regional seismic hazard information, such as possible scenarios and likelihood of destructive shaking intensity, and seismic vulnerability of structures, such as damage accumulation and loss generation [1–4]. Using probabilistic calculus, PSRA evaluates the potential damage and loss that a certain group of structures is likely to experience due to various seismic events. Two key components in PSRA are structural capacity modelling and seismic demand characterisation. A structural model that is used in the assessment is required to be capable of simulating a wide range of structural behaviour from damage initiation to collapse. In particular, realistic representation of ultimate damage states and failure modes is of critical importance. The complexity and hysteretic characteristics of structural systems in interaction with ground motions having different amplitudes and frequency content result in large uncertainty associated with seismic fragility. Several studies have attempted to quantify such uncertainty and assessed their impact on structural response prediction [5–7].

Parameterisation of earthquake damage and loss generation processes has major influence on the computation and modelling of EDP that is adopted as structural response variable for damage and loss assessment. Typical EDP parameters include the maximum ISDR and PFA for structural and non-structural components [8,9]. In addition to transient EDP parameters, residual ISDR may be a critical parameter in determining the usability of damaged structures in a post-earthquake situation [10–12]. In PSRA, EDP is either uni-variate or multi-variate. When a scalar parameter that correlates well with damage severity is employed, detailed probabilistic models are developed using seismic demand estimation methods, such as IDA [13]. The multi-variate case is often implemented using fragility models for different types of damage sensitivity (e.g. drift-sensitive versus acceleration-sensitive). However, fragility curves for different EDP parameters are evaluated separately and thus dependence of EDP variables for a given seismic intensity measure (IM; e.g. spectral acceleration) is not taken into account explicitly. Ruiz-Garcia and Miranda [14] and Ramirez and Miranda [9] highlighted that inclusion of residual drift as EDP, in addition to maximum ISDR and PFA, can have major impact on the economic consequence due to earthquake damage, because a

* Corresponding author.

http://dx.doi.org/10.1016/j.strusafe.2015.05.004
0167-4730/

severely-damaged building may be demolished due to expensive repair costs. Moreover, performance matrices based on both maximum and residual ISDRs (denoted by MaxISDR and ResISDR, respectively) have been proposed for use in seismic damage assessment [11]. It is noteworthy that in the above-mentioned studies, dependence of MaxISDR and ResISDR, which are physically inter-related and thus statistically correlated, has not been elaborated. Goda [15] and Uma et al. [16] investigated the joint probabilistic modelling of the two inter-related parameters using inelastic single-degree-of-freedom systems. However, rigorous evaluation of joint probability distributions of MaxISDR and ResISDR for realistic multi-degree-of-freedom systems has not been carried out. Therefore, further investigations of joint probabilistic modelling of multiple EDP parameters are warranted to consider different modes of damage and loss generation.

This study investigates the joint probabilistic modelling of multiple EDPs by conducting detailed characterisations of marginal probability distributions for MaxISDR, ResISDR, and PFA and copula models between MaxISDR and ResISDR. A copula technique offers a flexible way of describing nonlinear dependence among multi-variate data in isolation from their marginal probability distributions, and serves as a powerful tool for modelling nonlinearly-interrelated multi-variate data [17,18]. The method is applied to a 4-storey non-ductile RC building located in Victoria, British Columbia, Canada. Seismic vulnerability of pre-1970 buildings constructed in British Columbia remains to be a major concern because of the use of older design codes and poor construction practices (e.g. lack of column confinement and poor detailing) at the time of design and construction [19,20]. Moreover, Victoria is situated in an active seismic region, affected by complex regional seismicity due to shallow crustal earthquakes, deep inslab earthquakes, and mega-thrust Cascadia subduction earthquakes [21,22]. Seismic demand modelling is conducted based on IDA by developing a probabilistic relationship between IM and EDP. To avoid bias due to excessive record scaling in assessing seismic performance of a structure, a multiple conditional mean spectra (CMS) method is implemented by reflecting regional seismic hazard characteristics in British Columbia [23,24]. The developed multi-variate seismic demand model is then integrated with a storey-based damage–loss model for non-ductile RC frames [9] to evaluate the effects of incorporating ResISDR in PSRA and dependence modelling between MaxISDR and ResISDR on earthquake loss generation (including demolition). The novel contributions of this study are: (i) copula-based multi-variate modelling of EDP parameters is developed for a realistic structural model, and (ii) the impact of multi-variate seismic demand modelling is assessed in terms of expected seismic loss and seismic performance metrics. The former essentially extends the current IDA-based seismic demand modelling approaches.

The paper is organised as follows. A brief summary of copula modelling is presented in Section 2. Section 3 introduces an overall seismic risk analysis framework (Section 3.1), followed by descriptions of finite-element modelling of the 4-storey non-ductile RC frame (Section 3.2), regional seismic hazard information in British Columbia (Section 3.3), IDA and seismic demand modelling (Section 3.4), and storey-based damage–loss assessment (Section 3.5). In Section 4, results of multi-variate seismic demand modelling for the non-ductile RC frame in Victoria are discussed, and its effects on seismic loss are evaluated quantitatively. Finally, main conclusions from the investigations are mentioned in Section 5.

2. Dependence modelling using copulas

Consider the joint probability distribution of two random variables X_1 and X_2, $H(x_1,x_2) = P[X_1 \leqslant x_1, X_2 \leqslant x_2]$, continuous marginal probability distributions of which are denoted by $F_1(x_1)$ (=u_1) and $F_2(x_2)$ (=u_2), respectively. u_1 and u_2 represent a sample of a standard uniform random variable U_1 and U_2, respectively, and $P[\bullet]$ represents the probability. Sklar's theorem dictates that a relationship among $H(x_1,x_2)$, $F_1(x_1)$, and $F_2(x_2)$ can be established by using the copula function $C(u_1,u_2)$ [17]:

$$H(x_1,x_2) = C(F_1(x_1),F_2(x_2)) = C(u_1,u_2) \tag{1}$$

The joint probability distribution of the two random variables can be characterised by a copula function in terms of their marginal probability distributions. An important implication of this theorem is that marginal modelling and dependence modelling can be carried out separately.

For given data X_1 and X_2, their dependence can be characterised by the empirical copula $C^{\mathrm{E}}(u_1,u_2)$:

$$C^{\mathrm{E}}(u_1,u_2) = \frac{1}{N}\sum_{m=1}^{N} I\left(\frac{\mathrm{rank}(x_{1,m})}{N+1} \leqslant u_1, \frac{\mathrm{rank}(x_{2,m})}{N+1} \leqslant u_2\right) \tag{2}$$

where N is the total number of data, $I(\bullet)$ represents the indicator function, and $\mathrm{rank}(x_{1,m})$ (or $\mathrm{rank}(x_{2,m})$) is the rank of $x_{1,m}$ (or $x_{2,m}$) among x_1 (or x_2) in an ascending order. The empirical copula is a non-parametric description of dependence for a pair of random variables, which can be used for fitting various copula functions to data. A dependence measure that is suitable for copula modelling is the Kendall's τ coefficient:

$$\tau(X_1,X_2) = P\left[(X_1-\widetilde{X}_1)(X_2-\widetilde{X}_2)>0\right] - P\left[(X_1-\widetilde{X}_1)(X_2-\widetilde{X}_2)<0\right] \tag{3}$$

where $(\widetilde{X}_1,\widetilde{X}_2)$ is an independent copy of (X_1,X_2). The Kendall's τ measure is rank-dependent and invariant under strictly monotonic transformation.

In dealing with multi-variate data, the use of the normal and t copulas within a class of the elliptical copulas is popular. The bi-variate normal copula with the linear correlation coefficient ρ, $C_\rho^{\mathrm{N}}(u_1,u_2)$, is given by:

$$\begin{aligned} C_\rho^{\mathrm{N}}(u_1,u_2) &= \Phi_\rho(\Phi^{-1}(u_1),\Phi^{-1}(u_2)) \\ &= \int_{-\infty}^{\Phi^{-1}(u_1)}\int_{-\infty}^{\Phi^{-1}(u_2)} \frac{1}{2\pi\sqrt{1-\rho^2}}\exp\left(-\frac{s^2-2\rho st+t^2}{2(1-\rho^2)}\right)\mathrm{d}s\mathrm{d}t \end{aligned} \tag{4}$$

where $\Phi_\rho(\bullet)$ is the bi-variate standard normal distribution with ρ, and $\Phi^{-1}(\bullet)$ is the inverse standard normal distribution. The bi-variate t copula with ρ and the degree-of-freedom parameter ν, $C_{\rho,\nu}^t(u_1,u_2)$, is given by:

$$\begin{aligned} C_{\rho,\nu}^t(u_1,u_2) = t_{\rho,\nu}(t_\nu^{-1}(u_1),t_\nu^{-1}(u_2)) &= \int_{-\infty}^{t_\nu^{-1}(u_1)}\int_{-\infty}^{t_\nu^{-1}(u_2)} \\ &\times \frac{1}{2\pi\sqrt{1-\rho^2}}\left(1+\frac{s^2-2\rho st+t^2}{\nu(1-\rho^2)}\right)^{-(\nu+2)/2}\mathrm{d}s\mathrm{d}t \end{aligned} \tag{5}$$

where $t_{\rho,\nu}(\bullet)$ is the bi-variate t distribution with ρ and ν, and $t_\nu^{-1}(\bullet)$ is the inverse t distribution with ν. Both normal and t copulas are symmetrical, and the normal copula is a limiting case of the t copula when ν becomes infinity. The advantage of the t copula is that it can capture lower and upper tail dependence of data (i.e. joint non-exceedance and exceedance probabilities for rare events). For the t copula, the other parameter ν can be obtained by maximising the log-likelihood function.

Another widely-used copula family is the Archimedean copula. Popular Archimedean copulas include the Gumbel, Frank, and Clayton copulas, whose copula functions are given by:

$$C_\theta(u_1,u_2) = \exp\left(-\left[(-\ln u_1)^\theta + (-\ln u_2)^\theta\right]^{1/\theta}\right),\ \theta \geq 1 \tag{6}$$

$$C_\theta(u_1,u_2) = -\frac{1}{\theta}\ln\left(1+\frac{(\exp(-\theta u_1)-1)(\exp(-\theta u_2)-1)}{\exp(-\theta)-1}\right), \quad -\infty<\theta<\infty, \tag{7}$$

and,

$$C_\theta(u_1,u_2) = (u_1^{-\theta}+u_2^{-\theta}-1)^{-1/\theta}, \ \theta>1 \tag{8}$$

respectively. A distinction among these three copulas can be made with regard to the capability of capturing tail dependence: the Gumbel and Clayton copulas capture upper tail dependence and lower tail dependence, respectively, whereas the Frank copula shows no tail dependence. For the three copulas, the parameter θ can be estimated directly via $\tau(X_1,X_2)$. Alternatively, θ can be estimated based on the maximum log-likelihood method.

A limitation of using the above-mentioned copulas is the symmetrical property with respect to diagonal lines of a unit square (i.e. a domain defined by $[0,1]^2$). To deal with asymmetrical data in transformed space, a class of asymmetrical Archimedean copulas $C_{\theta,w1,w2}(u_1,u_2)$ can be used [17]:

$$C_{\theta,w_1,w_2}(u_1,u_2) = u_1^{1-w_1}u_2^{1-w_2}C_\theta(u_1^{w_1},u_2^{w_2}) \tag{9}$$

where w_1 and w_2 are the weight parameters and range from 0.0 to 1.0, and $C_\theta(u_1,u_2)$ represents the ordinary Archimedean copula. If $w_1 = w_2 = 1.0$, $C_{\theta,w1,w2}(u_1,u_2)$ equals the original Archimedean copula $C_\theta(u_1,u_2)$, while if $w_1 = w_2 = 0.0$, $C_{\theta,w1,w2}(u_1,u_2)$ equals the independence copula $C(u_1,u_2) = u_1u_2$. Various kinds of asymmetrical Archimedean copulas can be constructed by varying values of w_1 and w_2. The fitting of asymmetrical Archimedean copulas can be done based on the maximum likelihood method.

A suitable copula function can be selected quantitatively by comparing the evaluated values of the Akaike Information Criterion [25], which is defined as AIC = −2 × (sum of log-likelihood) + 2 × (number of parameters); a copula associated with the smallest AIC value is considered to be the best-fit copula. For illustration, several examples of simulated copula samples for the normal, *t*, Gumbel, Frank, Clayton, and asymmetrical Gumbel copulas are shown in Fig. 1.

3. Probabilistic seismic risk analysis

3.1. Seismic risk analysis methodology

Key consideration in modelling seismic damage and loss is proper treatment of uncertainty in quantifying seismic demand, structural capacity, and damage cost incurred due to unsatisfactory performance. The performance-based earthquake engineering (PBEE) methodology has been developed to assess seismic vulnerability of structures probabilistically [1–4]. Typically, an analytical procedure consists of hazard analysis, structural analysis, and damage–loss analysis. Mathematically, the PBEE methodology can be expressed based on total probability theorem [1]:

$$v(\mathrm{DV}) = \int\int G(\mathrm{DV}|\mathrm{EDP})\mathrm{d}G(\mathrm{EDP}|\mathrm{IM})|\mathrm{d}\lambda(\mathrm{IM})| \tag{10}$$

λ(IM) is the mean annual rate of exceeding a given IM level and is obtained from probabilistic seismic hazard analysis. The structural analysis develops a probabilistic relationship between IM and EDP, which is denoted by the complementary cumulative probability distribution function G(EDP|IM) in Eq. (10). The multi-variate seismic demand modelling that is carried out in this study is focused upon this component. It is based on IDA together with the multiple-CMS-based record selection (Section 3.4). The damage–loss analysis relates EDP to seismic performance metrics, parameterised with decision variables (DV), such as repair/reconstruction costs, downtime (loss of operability), and casualties. In Eq. (10), an intermediate step related to damage measures is suppressed because in this study, storey-based damage–loss (EDP–DV) functions [9] are employed (Section 3.5). It is also important to recognise that uncertainty enters the analysis at each step.

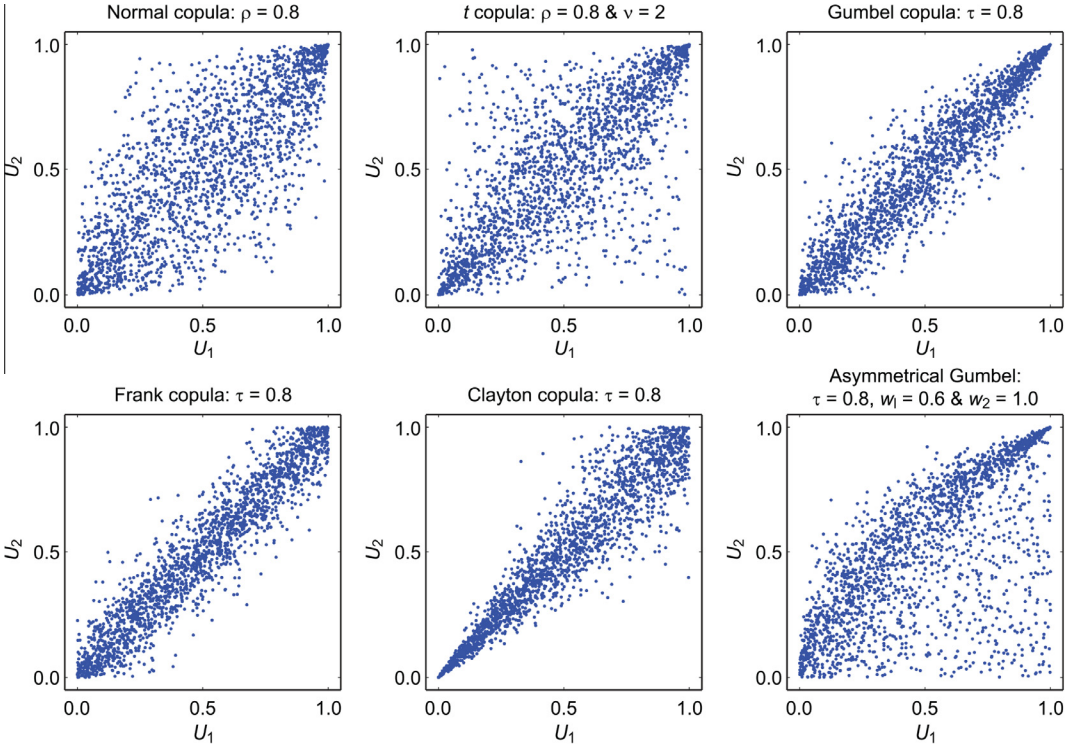

Fig. 1. Examples of simulated samples of the normal, *t*, Gumbel, Frank, Clayton, and asymmetrical Gumbel copulas.

The main variables in Eq. (10) can be multi-variate. The advantages of the multi-variate models are that the estimated quantities are less biased and have smaller uncertainty, which is accompanied by additional complexity in modelling efforts and implementation. In the PBEE framework developed in this study, a scalar IM (i.e. spectral acceleration at the fundamental vibration period) is considered. To achieve the sufficiency of IM [26], record selection is carried out using the multiple-CMS-based method [24], where earthquake characteristics in terms of magnitude, distance, spectral shape, and event type are taken into account, in addition to the information of spectral acceleration at the fundamental vibration period. The necessity for multiple EDP variables is directly attributed to damage–loss models adopted in this study. The EDP–DV functions by Ramirez and Miranda [9,12] involve three loss generation modes, i.e. non-collapse repair, collapse, and demolition, which are determined in terms of MaxISDR, ResISDR, and PFA at different storey levels (Section 3.5).

3.2. Structural model

A 4-storey RC space frame for office occupancy, which was designed and analysed by Liel and Deierlein [27], has a floor plan measuring 125 ft by 175 ft and columns spaced at 25 ft. The total height of the structure is 54 ft, having the storey heights at ground floor and at higher floor levels of 15 ft and 13 ft, respectively (Fig. 2a). The 1967 Uniform Building Code (UBC) seismic provisions [28] are applied; the design base shear coefficient is 0.068 g. The structure is designed as a space frame, such that all columns and beams are part of the lateral resisting system, having concrete strength f_c = 27.6 MPa and reinforcing bar strength f_y = 413.7 MPa in both beams and columns. All beam and column elements have the same amount of over-strength, such that each element is 15% stronger than the code-minimum design level. The design is governed by strength and stiffness requirements, as the 1967 UBC had few requirements for special seismic design or ductile detailing.

Finite-element modelling of a structure can be achieved through a fibre or lumped plasticity model. In the fibre model, the element cross-section is discretised and corresponding non-linear material properties of the core concrete, cover concrete, and reinforcing bars are assigned. On the other hand, in the lumped plasticity model, non-linearity of the beam-column element is introduced at the two ends (hinges), which are connected by an elastic element. The investigations carried out by Haselton et al. [29] indicate that the lumped plasticity model, equipped with adequate hysteretic models for plastic hinges, can simulate global collapse behaviour well, whereas the fibre model may be numerically unstable when the responses become highly nonlinear. The non-ductile structure by Liel and Deierlein [27] is modelled through the lumped plasticity concept. The lumped plasticity element models used to simulate plastic hinges in beam-column elements adopt a nonlinear spring model developed by Ibarra et al. [30]. This model is capable of capturing important modes of deterioration that lead to side-sway collapse of RC frames. Fig. 2b shows a tri-linear monotonic backbone curve of the plastic hinge model. The detail of calibration of model parameters can be found in [27,29]. Modal analysis of the finite-element model indicates that the first three modal periods of the 4-storey frame are 1.92, 0.55, and 0.27 s, respectively. For this structure, spectral acceleration at 2.0 s is adopted as IM, while MaxISDR, ResISDR, and PFA at ground floor are selected as EDP. In the developed approach that is explained later, EDP variables at storey levels above the ground floor are approximated using response shape function over the height of the structure; this introduces additional uncertainty in characterising these EDP variables. The focus upon structural responses at ground floor as key EDP variables is justified because the storey height at the base is greater than other floor levels and thus the structure tends to fail in a soft-storey sway mechanism (Section 4.1).

3.3. Seismic hazard and ground motion in British Columbia, Canada

A case study site is focused upon Victoria, where non-seismically designed vulnerable RC frames exist and are still in use. There are mainly three potential sources of damaging earthquakes in British Columbia: shallow crustal earthquakes, deep inslab earthquakes, and off-shore mega-thrust interface earthquakes from the Cascadia subduction zone [21]. The expected moment magnitude (M_w) of the Cascadia events is in the range of 8–9; its mean recurrence period ranges from 500 to 600 years and the last event occurred in 1700. In this study, an updated regional seismic hazard model by Atkinson and Goda [22] is adopted to characterise seismic hazard in Victoria (site condition is set to site class C). Fig. 3 shows uniform hazard spectra (UHS) and seismic deaggregation results for Victoria from probabilistic seismic hazard analysis. Two return period levels, i.e. 500 and 2500 years, are considered, and the spectral period for seismic deaggregation results is set to 2.0 s, which is close to the fundamental vibration period of the 4-storey non-ductile RC frame. It is important to recognise that the hazard estimates are based on numerous earthquake scenarios that may occur in a seismic region of interest, and different earthquake types are associated with

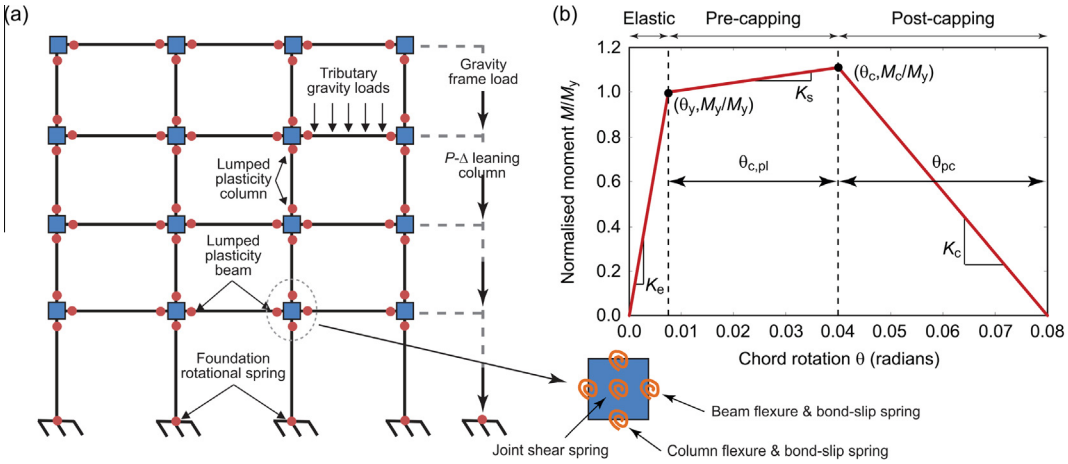

Fig. 2. (a) Nonlinear finite-element model of 4-storey non-ductile RC frame and (b) backbone curve of Ibarra element model used for beam-column elements.

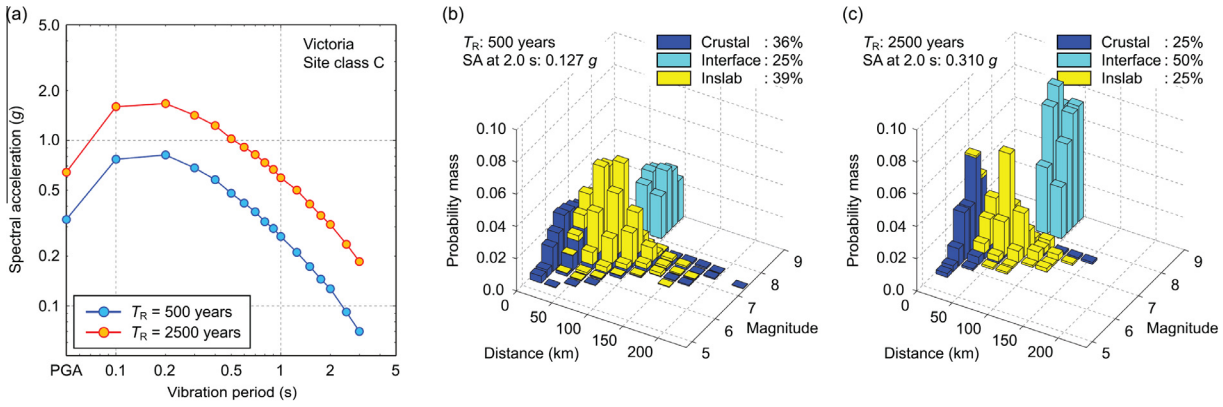

Fig. 3. Probabilistic seismic hazard results for Victoria (site class C): (a) UHS at return periods of 500 and 2500 years, (b) seismic deaggregation at return period of 500 years, and (c) seismic deaggregation at return period of 2500 years.

distinct event features in terms of magnitude and distance. With the increase of return period, relative contributions from the Cascadia events increase; for instance, at the return period of 2500 years, 50% of the dominant scenarios are originated from the mega-thrust subduction zone. This is an important consideration in selecting records for seismic performance evaluation of (relatively flexible) structures in Victoria.

The input ground motion records for use in IDA need to be selected carefully, because record scaling, as implemented in IDA, may induce bias in calculated structural responses [31]. It is also important that selected time-histories have similar record characteristics (e.g. magnitude, duration, and spectral shape) as target seismic hazard. For this purpose, a new ground motion database has been compiled by including recent recordings from Japan, in particular, the 2011 M_w9 Tohoku earthquake records. The Tohoku dataset is relevant to the Cascadia event, because of anticipated macro-level similarity between these two mega-thrust subduction events, which is not present in ground motion data from other smaller earthquakes. The new ground motion database combines recordings from the Next Generation Attenuation dataset and from three national/regional ground motion networks in Japan, i.e. K-NET, KiK-net, and SK-net. An innovative aspect of the database is that all time-history data are associated with actual mainshock–aftershock sequences, and is an extended version of those developed by Goda and Taylor [32] and Goda [33]. The combined database is comprised of 606 mainshock–aftershock record sequences; mainshocks within individual sequences are identified as events having the largest earthquake magnitude, and all mainshock records have moment magnitudes greater than 5.9, rupture distances less than 300 km, and peak ground acceleration greater than 75 cm/s^2. In this study, mainshock records are focused upon (note: seismic demand modelling for mainshock–aftershock sequences is reported in [34]).

3.4. Record selection and incremental dynamic analysis

Using the constructed ground motion database, 50 records (two horizontal components per record; i.e. 100 time-histories) are selected based on the multiple CMS method [24]. The target CMS for three earthquake types (crustal/interface/inslab) are derived from probabilistic seismic hazard analysis (Fig. 3), and response spectra of the selected records match the target CMS over the vibration period range between 0.3 and 3.0 s in a least squares sense. The number of records for each earthquake type, out of 50 records, is determined based on its relative contribution to seismic hazard using deaggregation results. Specifically, at the return period of 2500 years, the number of records for crustal, interface, and inslab events is 13, 25, and 12, respectively. Fig. 4 compares UHS and CMS for three event types for Victoria at the return period of 2500 years. In addition, the figure shows the magnitude–distance distribution of the selected 50 records. The CMS are usually lower than the corresponding UHS. The response spectral shape for

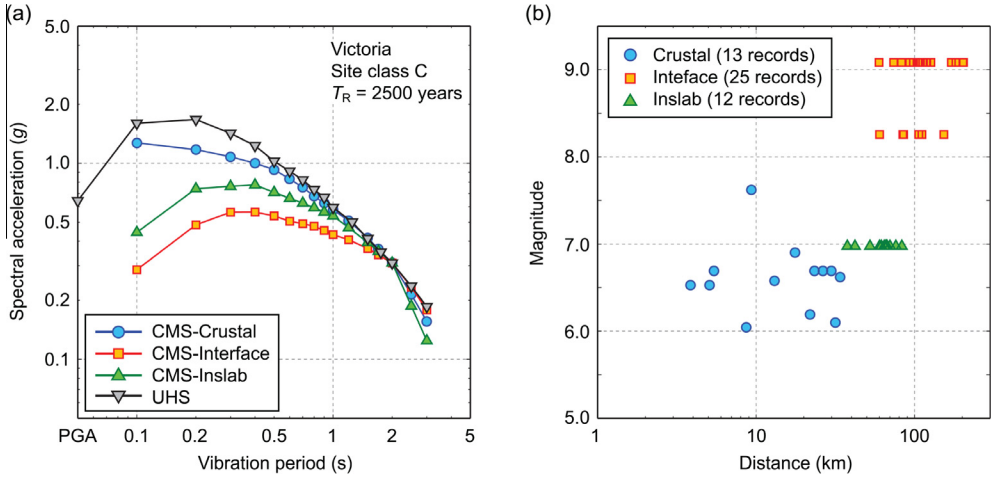

Fig. 4. (a) Comparison of CMS for crustal, interface, and inslab events with UHS for Victoria at return period of 2500 years, and (b) magnitude–distance plot of the selected 50 records.

crustal events tends to have more spectral content in the short vibration period range (i.e. slope becomes steeper), while that for interface events tends to be flatter (i.e. more relative frequency content in the long vibration period).

IDA is carried out for the 4-storey non-ductile RC frame using the set of 50 records. The seismic intensity level (i.e. IM) ranges from 0.05 to 0.7 g (in total, 30 levels). For each nonlinear dynamic analysis, MaxISDR, ResISDR, and PFA at all storey levels are stored for post-processing. In general, numerical instability is encountered when ISDR of the frame exceeds 0.10. The first occurrence of such large-deformation responses in terms of seismic intensity level is treated as 'collapse' in this study. This definition of collapse capacity is consistent with [13].

Fig. 5a shows a collapse fragility curve obtained from IDA results (raw data and fitted lognormal curve). The majority of collapse occurs at seismic intensity between 0.2 and 0.4 g. The parameters of the collapse fragility curve are: median = 0.28 g and logarithmic standard deviation = 0.38. It is noted that modelling uncertainties related to structural capacities [5] are not included in the logarithmic standard deviation. Moreover, Fig. 5b displays four cases of damage state limits for demolition, which are based on the lognormal probability distribution. The models are expressed as a function of ResISDR. When ResISDR exceeds the demolition damage state threshold, a damaged structure is demolished, rather than repaired. Ramirez and Miranda [12] used median of 0.015 and logarithmic standard deviation of 0.3 as a base case, noting that this is based on expert opinion, rather than quantitative investigations.

The main IDA results for MaxISDR, ResISDR, and PFA (ground floor) are shown in Fig. 6. To present the uncertainty of the IDA results succinctly, two sets of percentile curves, i.e. 16th–84th curves and 2.5th–97.5th curves, are included in the figure. The two sets approximately correspond to mean plus/minus one standard deviation and mean plus/minus two standard deviations. The results shown in Fig. 6 suggest that the overall characteristics of the IDA curves for MaxISDR and ResISDR are different; the former increases gradually with the seismic intensity level, while the latter increases rapidly when the seismic intensity level reaches about 0.15 g (at which the corresponding median MaxISDR is about 0.025). The results, in light of possible demolition damage state limit curves shown in Fig. 5b, suggest that for some cases, non-collapse structure may be demolished. It is noteworthy that the uncertainty of ResISDR is much greater than that of MaxISDR (as noted by Ruiz-Garcia and Miranda [14]). The IDA results for PFA show linear trends. Looking at the EDP–DV functions for the non-ductile RC frame (Section 3.5), impact due to acceleration may be less significant in comparison with that due to drift. The IDA results shown in Fig. 6 only illustrate marginal probabilistic characteristics of EDP parameters as a function of IM. Their joint characteristics are investigated and modelled in Section 4.

3.5. Storey-based damage–loss functions

The damage–loss analysis relates EDP to DV through probabilistic loss models $G(\mathrm{DV}|\mathrm{EDP})$. In this study, following the storey-based damage–loss models [9], building components are lumped into

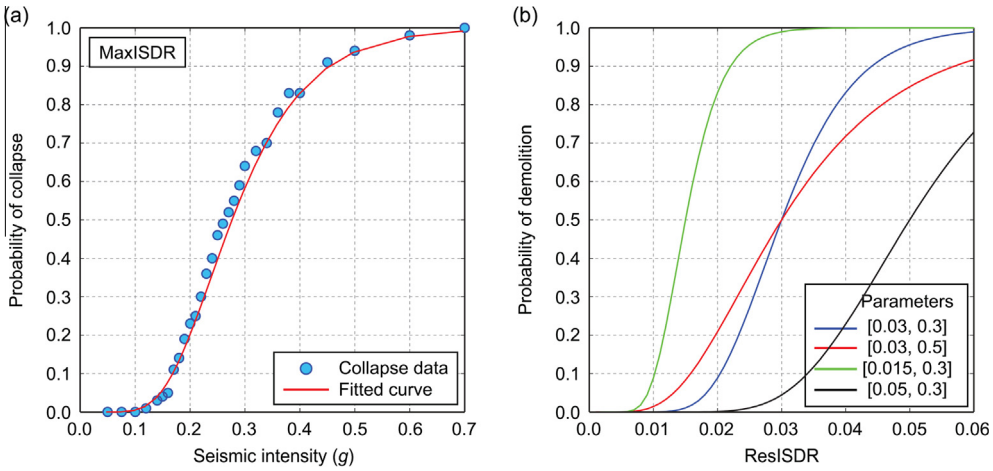

Fig. 5. (a) Collapse fragility function, and (b) demolition damage state limit curves (parameters are median and logarithmic standard deviation).

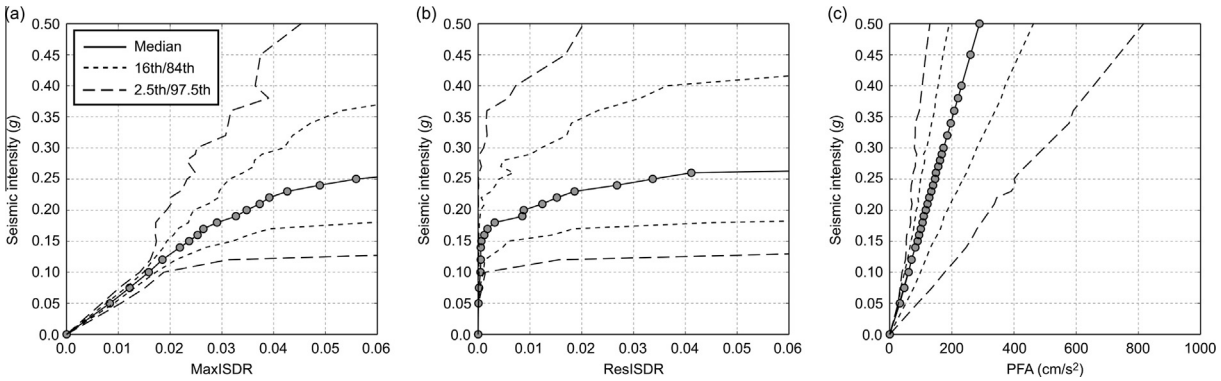

Fig. 6. Incremental dynamic analysis results: (a) MaxISDR, (b) ResISDR, and (c) PFA. The EDPs are at ground floor.

groups based on component type (e.g. structural elements and interior partitions), location within a building (e.g. storey level), and relevant EDP (i.e. damage sensitivity). DV that is concerned in this study is direct economic loss (building repair/replacement costs); other seismic losses due to business interruption and relocation are not included. The formulation of the storey-based seismic loss estimation simplifies a process of calculating seismic loss (i.e. DV) as a function of EDP, and it requires less information on structural details and their costs, in comparison with a rigorous assembly-based seismic loss approach [8]. The original EDP–DV functions [9] are developed for 9 component-storey combinations: three categories, i.e. drift-sensitive structural components (e.g. beam/slab-column subassembly), drift-sensitive non-structural components (e.g. partitions and windows), and acceleration-sensitive non-structural components (e.g. ceilings and ventilation systems), and three storey classes, i.e. ground floor, typical floor, and top floor. The distinction of the building storey level stems from different building layout and use at different levels (which affect proportions of incurred seismic damage costs for different building components).

The seismic loss L_T for given EDP can be expressed as [12]:

$$L_T = L_{NC} + L_D + L_C \tag{11}$$

where L_{NC}, L_D, and L_C are the seismic losses for non-collapse repairs (NC), demolition (D), and collapse (C) cases, respectively. The three situations are disjoint and mutually exclusive. The numerical evaluation of L_T in PSRA calculations is facilitated as follows: (i) collapse probability is assessed for MaxISDR (Fig. 5a); if collapse is predicted, then $L_T = L_C$; (ii) demolition of the structure is determined according to a realised value of ResISDR in comparison with the (uncertain) limit state function for demolition (Fig. 5b); if demolition is predicted, then $L_T = L_D$; and (iii) otherwise, L_{NC} is assessed by using EDP–DV functions for non-collapse cases. It is noted that L_{NC}, L_D, and L_C are random variables. The demolition and collapse (replacement) costs L_D and L_C can be simulated as lognormal variable, having the median cost of μ_{LD} and μ_{LC} and the coefficient of variation (CoV) of v_{LD} and v_{LC}, respectively. The median demolition and replacement costs can be estimated using mean unit-area construction cost and total floor area. The values for v_{LD} and v_{LC} can be adopted from the literature (e.g. [35]), which ranges widely from 0.2 to 1.1; typically, 0.6–0.7 appears to be reasonable for general situations.

The evaluation of L_{NC} in Eq. (11) is conducted using EDP–DV functions. Although mean EDP–DV functions for 9 component-storey combinations are provided by Ramirez and Miranda [9], no ready-to-use equations for CoV are given. As it is important to consider all major uncertainties in PSRA, CoV estimates of the EDP–DV functions are obtained using available information of fragility and damage cost as provided in [9]. The derived EDP–DV functions are for 27 subcontractor-sensitivity-storey combinations (i.e. 9 subcontractor-sensitivity combinations and ground/typical/-top). The subcontractor classification is concrete/metal/doors–windows–glass/finishes/electrical/mechanical, and the concrete/metal/doors–windows–glass category is applicable to drift-sensitive components only (i.e. 6 subcontractor-sensitivity categories for drift-sensitive components while 3 subcontractor-sensitivity categories for acceleration-sensitive components). This elaboration is necessary because information of cost variability is available for a subcontractor basis only. Fig. 7 shows mean EDP–DV functions for 9 subcontractor-sensitivity combinations at ground floor (normalised by storey-level loss). The corresponding CoV values are indicated in the figure legend.

4. Multi-variate seismic demand modelling

Joint probabilistic modelling of MaxISDR, ResISDR, and PFA is performed. Firstly, preliminary analysis results of the calculated EDP parameters are presented in Section 4.1 to identify a suitable approach for characterising multi-variate data. The marginal and dependence modelling of MaxISDR, ResISDR, and PFA is carried out in Section 4.2 to develop multi-variate seismic demand prediction models. In Section 4.3, IM–DV functions are developed by integrating IM–EDP seismic demand models with EDP–DV functions.

4.1. Preliminary analysis

The aim of the preliminary analysis is to identify the key EDP parameters in developing inelastic seismic demand prediction models. There are 12 parameters: MaxISDR, ResISDR, and PFA at four storey levels. It is necessary to reduce the number of the parameters as joint probabilistic modelling of 12 random variables is challenging (except for the case of multivariate normal/lognormal distribution). Because the consideration of MaxISDR, ResISDR, and PFA is essential from a standpoint of damage–loss analysis (Section 3.5), it is important to determine which storey level to focus on. The building height variation between 15 ft (ground floor) and 13 ft (second and higher floors) introduces stiffness difference (≈65%). This is constituted as soft storey floor [36], and consequently, the demand at this floor will dominate. Fig. 8 shows normalised response ratios of MaxISDR, ResISDR, and PFA

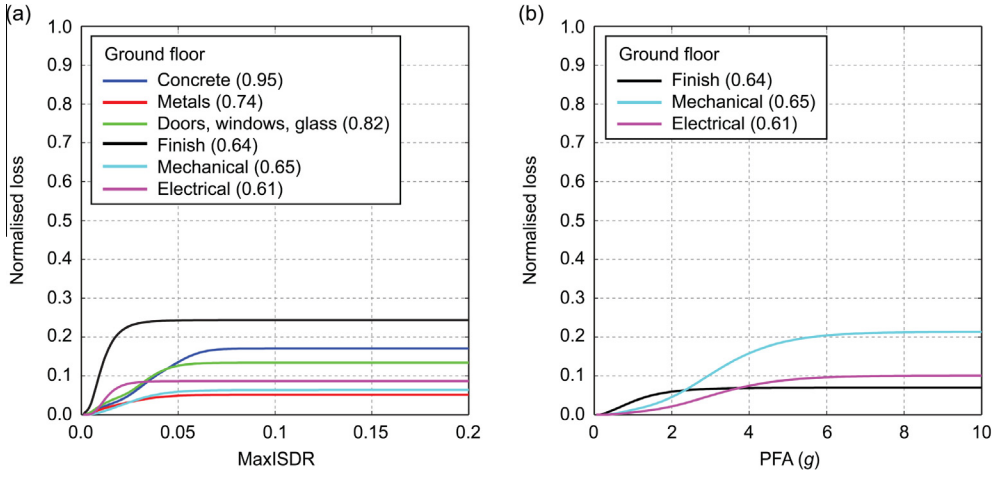

Fig. 7. EDP–DV functions for 9 subcontractor-sensitivity combinations (ground floor). The number inside parentheses is the CoV of the EDP–DV function.

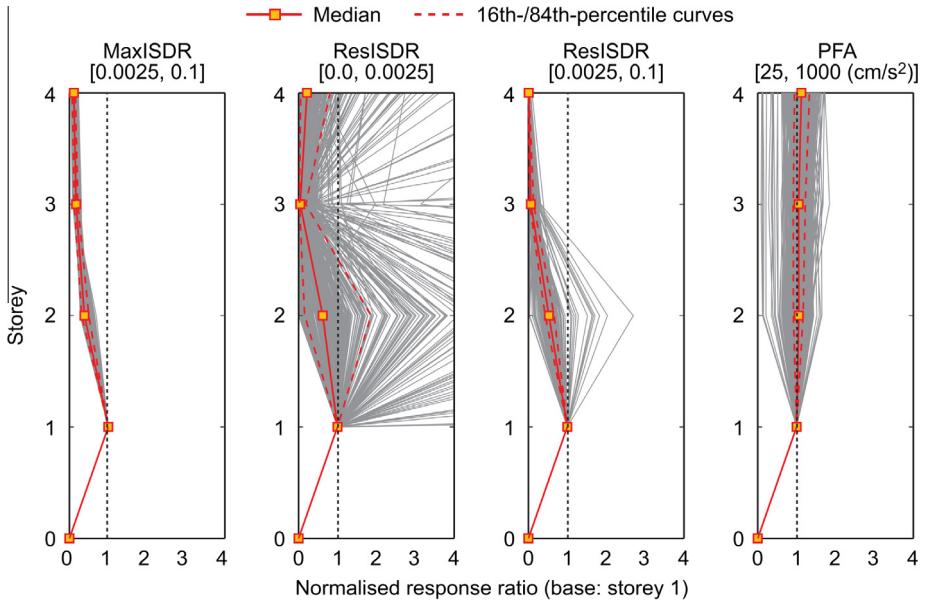

Fig. 8. Normalised response ratios for MaxISDR, ResISDR (two ISDR ranges: [0.0, 0.0025] and [0.0025, 0.1]), and PFA.

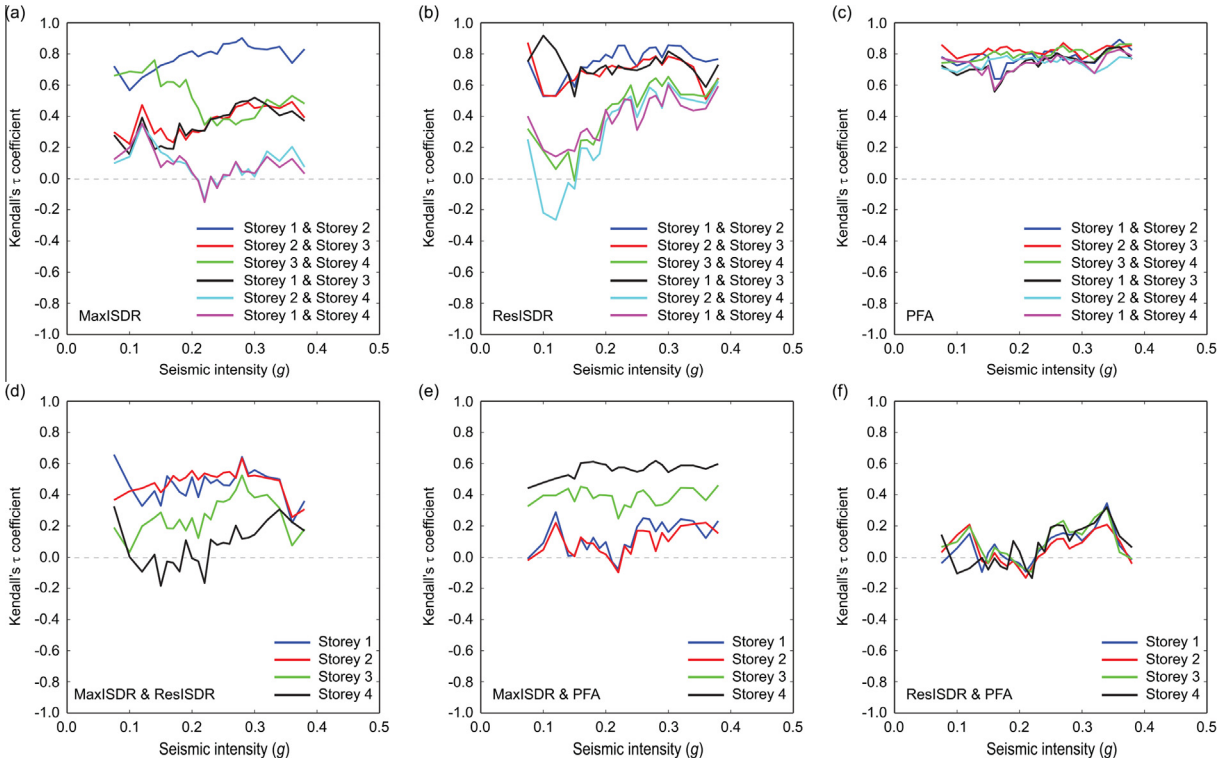

Fig. 9. Kendall's τ coefficients for MaxISDR, ResISDR, and PFA by considering the same EDP parameters at different storey levels (a–c) and different EDP parameters at the same storey levels (d–f).

with respect to the response at ground floor (i.e. response shape function); for PFA, the shape functions are developed based on the acceleration responses at the ceiling/roof height for individual storeys. For ResISDR, the shape functions are developed for two ISDR ranges, i.e. [0.0,0.0025] and [0.0025,0.1], to inspect the shape functions in terms of response level. Fig. 8 indicates that: (i) the shape function for MaxISDR is stable across different response levels and has the maximum at ground floor, the latter reflecting a typical failure mode of the non-ductile RC frame, i.e. column hinging at low storey levels; (ii) the shape function for ResISDR at the small response level is highly variable due to its high sensitivity when the structure behaves elastically, whereas that at the moderate-to-large response level has more common trends with moderate variability; and (iii) the shape function for PFA is similar at different response levels, involving moderate degrees of variability (e.g. 0.5–1.5 with respect to the PFA response at ground floor).

To quantify the correlation of EDP parameters at different storey levels, the Kendall's τ coefficient is evaluated and presented for the same EDP parameter at different storey levels (Fig. 9a–c) and for different combinations of EDP parameters at the same

storey level (Fig. 9d–f). The results are shown for the cases where a sufficient number of non-collapse data points are available for the calculation of the τ coefficient (i.e. 25 samples). Fig. 9 shows that when two storey levels are physically close the correlation tends to be higher, and that PFA responses at different storey levels are more correlated in a consistent manner than MaxISDR and ResISDR. The correlation for MaxISDR and ResISDR at storey level 1 or 2 is moderate, although such correlation is not clear at higher storey levels. A different trend is observed for MaxISDR and PFA; the correlation tends to increase with the storey level. For ResISDR and PFA, the degree of dependence is low.

Based on the results presented in Figs. 8 and 9, it is decided that three parameters, MaxISDR, ResISDR, and PFA at ground floor, are focused upon in multi-variate seismic demand modelling. This selection is consistent with the expected failure mode of the non-ductile structure. Given the values of MaxISDR, ResISDR, and PFA at ground floor (i.e. storey 1 in Fig. 8), response values at upper floors can be obtained (or sampled) by using the response shape factors (Fig. 8) together with the correlation coefficients (Fig. 9). In the following, joint modelling of the three primary EDP parameters is examined further. Specifically, MaxISDR and ResISDR are treated as dependent random variables, while PFA is modelled as an independent one.

4.2. Marginal and dependence modelling of engineering demand parameters

Marginal distribution modelling of MaxISDR, ResISDR, and PFA at ground floor is carried out. First, suitable marginal probability distribution types for MaxISDR, ResISDR, and PFA are examined. Previous studies (e.g. [15]) suggest that the lognormal and Frechet distributions are adequate for MaxISDR, whereas ResISDR has a heavy right tail. To investigate this problem, six probability distributions, namely, lognormal, Gumbel, Frechet, Weibull, gamma, and generalised Pareto, are used for marginal probability distribution modelling of the three EDP parameters. The model selection is conducted by inspecting quantile–quantile (Q–Q) plots and by comparing the calculated log-likelihood values (which is an indicator for model fitness, noting that the number of model parameters for these distributions is the same (=2); for the generalised Pareto distribution, the shift parameter is set to 0.0025). The Q–Q plots for MaxISDR, ResISDR, and PFA at seismic intensity levels of 0.15 and 0.25 g are shown in Fig. 10; for MaxISDR and PFA, the lognormal and Frechet distributions are chosen for illustration, while for ResISDR, the generalised Pareto and gamma distributions are considered. By examining similar plots at different seismic intensity levels and log-likelihood values, it is concluded that the Frechet distribution may be used for MaxISDR and PFA (note: the lognormal distribution performs well) and the generalised Pareto distribution may be chosen for ResISDR. It is noteworthy that the identified marginal distributions for the three EDP parameters are non-normal (in particular, ResISDR); in such cases, conventional multi-variate normal/lognormal distribution modelling is not ideal (e.g. [37]), and a more elaborated approach is preferred.

Next, copula modelling of MaxISDR and ResISDR is carried out. To illustrate the data characteristics of the two parameters, scatter plots of original data and transformed data at seismic intensity levels of 0.15 and 0.25 g are presented in Fig. 11. The transformed data (i.e. empirical copula samples) are obtained based on ranked and sorted data (Eq. (2)). The visual inspection of the scatter plots indicates that MaxISDR and ResISDR are dependent and that upper tail dependence of the transformed data is appreciable (i.e. concentration of transformed data points in the upper-right corner). To model the observed dependence of MaxISDR and ResISDR, parametric copula functions are fitted to empirical copula samples using the maximum likelihood method [17]. The parametric copulas that are considered in this study include: normal, t, Frank, Gumbel, Clayton, and asymmetrical Archimedean copulas (Section 2). The copula fitting of MaxISDR and ResISDR at various seismic intensity levels suggests that overall the asymmetrical Gumbel copula is suitable for the majority of the cases examined in this study.

The final model component for probabilistic seismic demand modelling is to develop prediction equations for parameters of the marginal distribution functions and copula functions for a wide range of IM levels (note: the model fitting above is carried out at discrete 30 IM levels, whereas parameters at IM values that are not considered in IDA are required in PSRA). For marginal distributions of MaxISDR, ResISDR, and PFA, mean and standard deviation

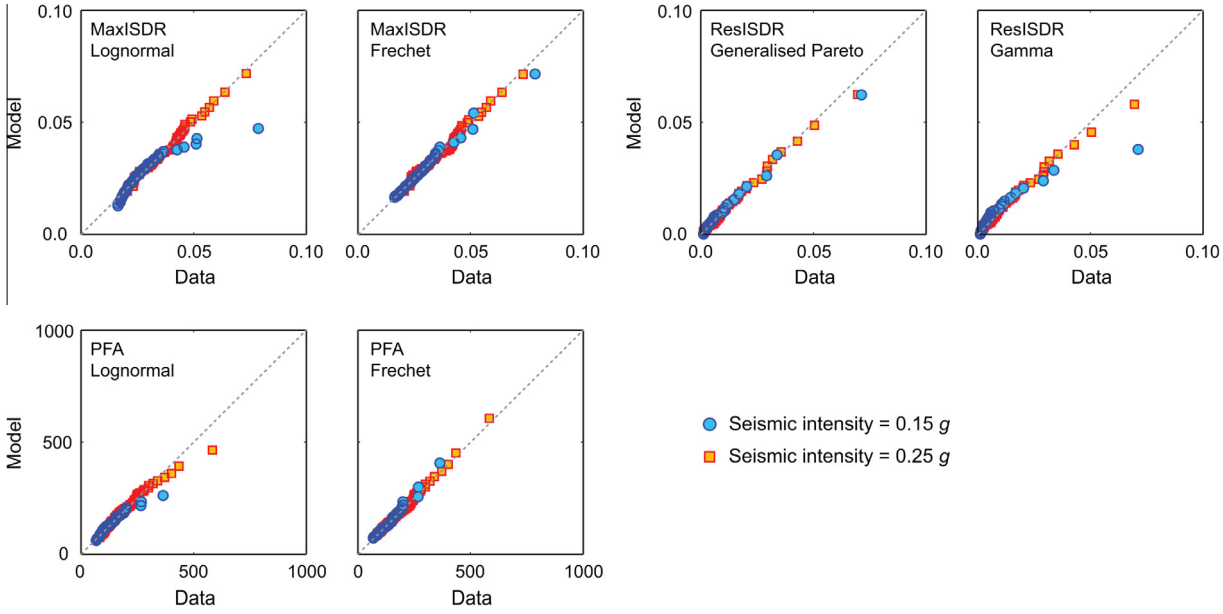

Fig. 10. Quantile–quantile plots for MaxISDR, ResISDR, and PFA at seismic intensity levels of 0.15 and 0.25 g (the lognormal and Frechet distributions are used for MaxISDR and PFA, whereas the generalised Pareto and gamma distributions are used for ResISDR).

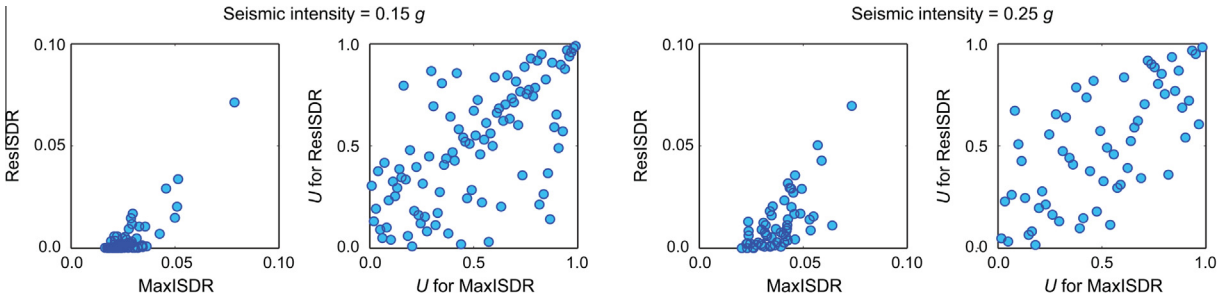

Fig. 11. MaxISDR–ResISDR scatter plots (original and transformed data) at seismic intensity levels of 0.15 and 0.25 *g*.

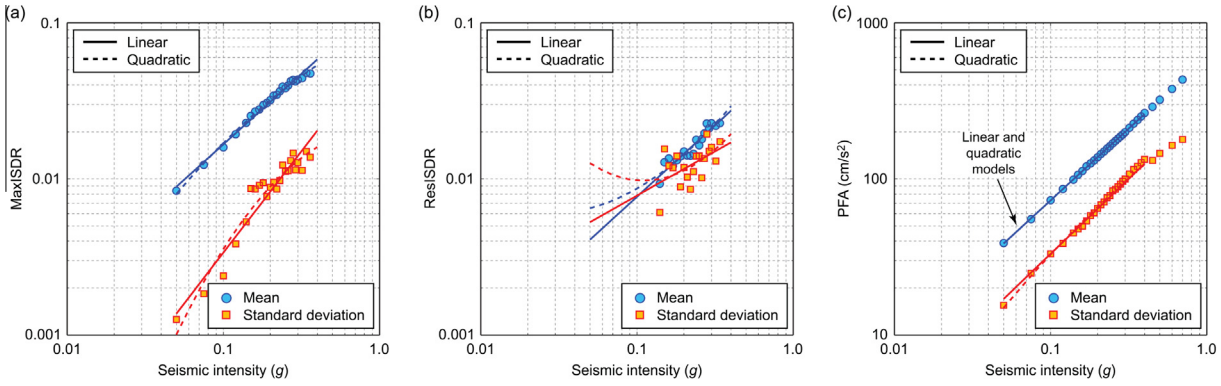

Fig. 12. Curve fitting to mean and standard deviation of EDP parameters: (a) MaxISDR, (b) ResISDR, and (c) PFA.

need to be characterised. On the other hand, for the dependence modelling of MaxISDR and ResISDR, three parameters of the asymmetrical Gumbel copula and the Kendall's τ coefficient need to be fitted using mathematical functions. Fig. 12 shows the curve fitting results of the mean and standard deviation of MaxISDR, ResISDR, and PFA as a function of IM. In conducting the fitting exercise, several functional forms, linear and quadratic functional forms and linear IM and logarithmic IM, have been tested. For MaxISDR (Fig. 12a), both linear and quadratic functions work well for the mean and standard deviation (the quadratic equations are adopted). For ResISDR (Fig. 12b), the linear function provides a more robust trend outside of the data range than the quadratic function, and is appropriate for use in PSRA. The equations for PFA (Fig. 12c) exhibit linear trends over a wide range of IM. Overall, both linear and quadratic functions fit the data well (the quadratic equations are adopted). The comparison of the CoV values for MaxISDR, ResISDR, and PFA (which are not shown directly, but can be appreciated by inspecting the differences between mean and standard deviation) provides quantitative information of the variability of the EDP variables. The CoV for MaxISDR ranges between 0.1 and 0.4, and that for PFA is relatively stable ranging between 0.4 and 0.5. On the other hand, the CoV for ResISDR ranges between 0.5 and 1.2 and has a decreasing tendency with respect to IM; large CoV values at low IM levels reflect the significant sensitivity of this variable, when the structure behaves elastically. The main features of the three EDP variables can be captured by using the developed equations for the statistics.

Fig. 13 shows the curve fitting to the Kendall's τ coefficient and two parameters (θ and w_1) of the asymmetrical Gumbel copula ($w_2 = 1.0$ for all cases). The former can be used to estimate the copula parameters for the normal, *t*, and other Archimedean copulas. Generally, scatter of the data points is large compared with the statistics of MaxISDR, ResISDR, and PFA (Fig. 12). Based on the obtained results, it is decided that constant models are appropriate for the copula parameters.

To examine accuracy of the joint probabilistic modelling of MaxISDR, ResISDR, and PFA at ground floor, simulated samples of these variables are compared with the IDA results for various seismic intensity levels. The size of simulated samples for a given IM level is 1000. To evaluate the similarity/dissimilarity of the simulated samples with the original IDA data, the two-sample Kolmogorov–Smirnov test is carried out at a significance level of 0.1. The null hypothesis is that the simulated samples and the original data are from the same probability distribution. For the majority of the cases where sufficient data points are available for probabilistic modelling, the null hypothesis cannot be rejected. The exception includes the low IM level cases for which the model parameters of the marginal probability distributions are not well constrained. Overall, it is concluded that the marginal distribution modelling of MaxISDR, ResISDR, and PFA is satisfactory.

Next, performance of dependence modelling for MaxISDR and ResISDR pairs is examined. For this purpose, three fitted copula functions, i.e. asymmetrical Gumbel copula, normal copula, and independence copula, are considered, and scatter plots of MaxISDR and ResISDR based on the IDA results and simulated samples at seismic intensity levels of 0.15 and 0.25 *g* are compared in Fig. 14. Note that the marginal distribution modelling is identical for the three cases. Thus differences of the MaxISDR and ResISDR data pairs are attributed to the copula functions alone.

The results for the asymmetrical Gumbel copula indicate that the general features of the simulated samples resemble those of the original data. For some cases, there are 'unrealistic' pairs (i.e. ResISDR exceeds MaxISDR); the boundary between realistic and unrealistic cases is shown by a dotted line. Typically, 1–4% of the samples may fall into unrealistic cases (note: although these pairs are not physically possible, the difference between ResISDR and MaxISDR is not large, distributed around the boundary line). In PSRA, such unrealistic cases can be avoided by simply adopting physically possible MaxISDR–ResISDR pairs only. The results based on the normal copula show that generally, the upper tail

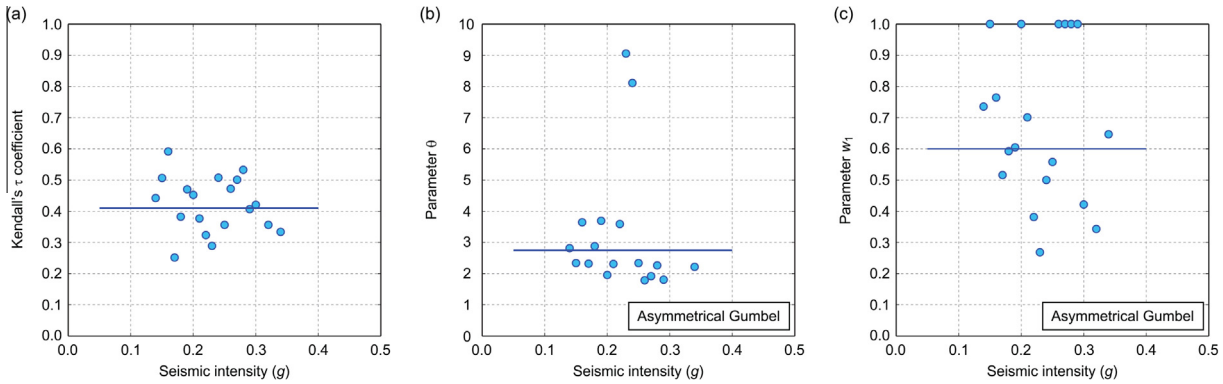

Fig. 13. Curve fitting to the Kendall's τ coefficient (a) and the model parameters θ and w_1 of the asymmetrical Gumbel copula (b and c) (w_2 is set to 1).

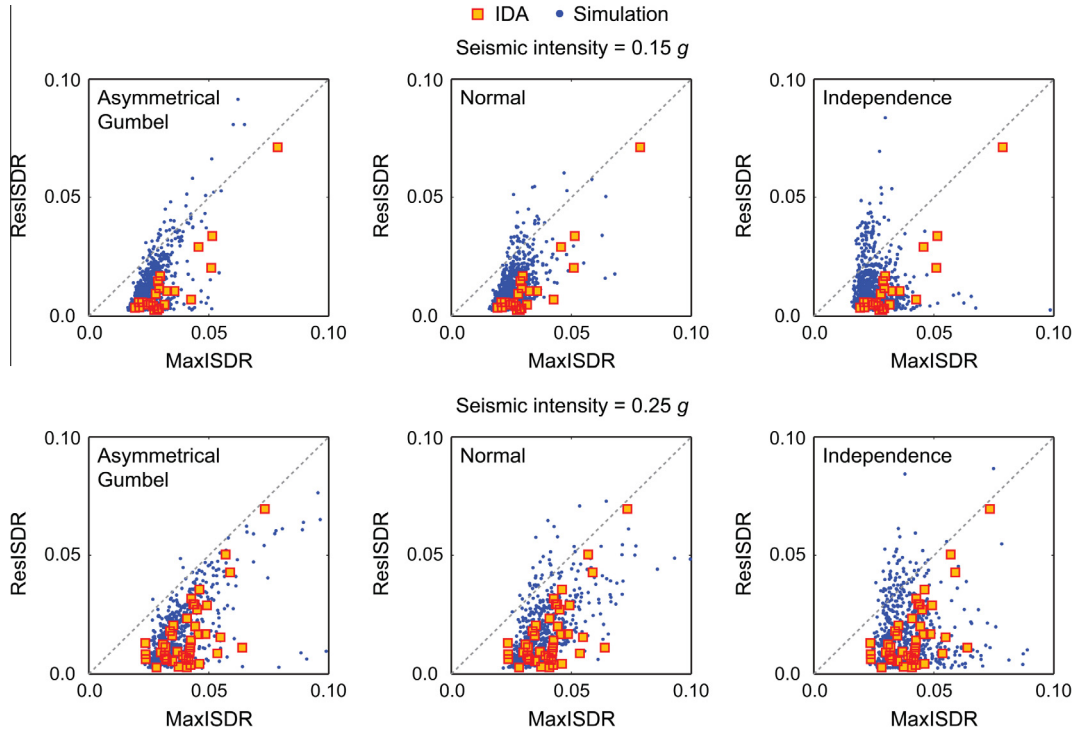

Fig. 14. Comparison of MaxISDR–ResISDR scatter plots based on the IDA results and simulated samples at seismic intensity levels of 0.15 and 0.25 g by considering the asymmetrical Gumbel, normal, and independence copulas.

characteristics of the original data are captured well. The chance of generating unrealistic pairs is similar to that for the asymmetrical Gumbel copula (i.e. typically, 1–4%). When the correlation coefficient is relatively high, the data points are concentrated along the diagonal line in the transformed space (Fig. 1); this decreases the chance of having copula samples in the off-diagonal corners. Different features of the MaxISDR–ResISDR pairs can be seen in the lower part of the scatter plots; not many samples are generated for large MaxISDR and small ResISDR cases (which can occur in real situations). This is one of the reasons that the normal copula is associated with larger AIC values in model selection (thus not preferred). However, this difference may not have major impact on the calculated seismic loss because large seismic demand cases have more impact on the seismic loss. Moreover, the results for the independence copula indicate that the upper tail characteristics of the original data are not captured by the simulated samples, and occurrence of unrealistic pairs is much more frequent than the asymmetrical Gumbel and normal copulas. Therefore, the independence copula is not suitable in PSRA.

4.3. Comparison of seismic loss ratios (IM–DV functions)

To verify that the fitted statistical models produce reasonable estimates of the EDP parameters, the developed multi-variate seismic demand models (i.e. IM–EDP functions; Section 4.2) as well as storey-based damage–loss models (i.e. EDP–DV functions; Section 3.5) are implemented in Monte Carlo simulation. This facilitates the construction of IM–DV functions for different types of seismic failure modes (i.e. collapse, demolition, and non-collapse damage; Eq. (11)).

The mean IM–DV functions are developed by generating 10,000 samples of (normalised) seismic damage costs for each IM level. Fig. 15 compares four IM–DV functions for collapse, demolition, non-collapse loss, and total loss by considering different copula models (with the demolition damage limit state parameters = [0.03,0.3]) (Fig. 15a) and different demolition parameters = [0.03, 0.5], [0.015, 0.3], and [0.03, 0.5] (Fig. 15b–d). The comparison of the IM–DV functions for demolition based on different copula models shown in Fig. 15a indicates that the IM–DV

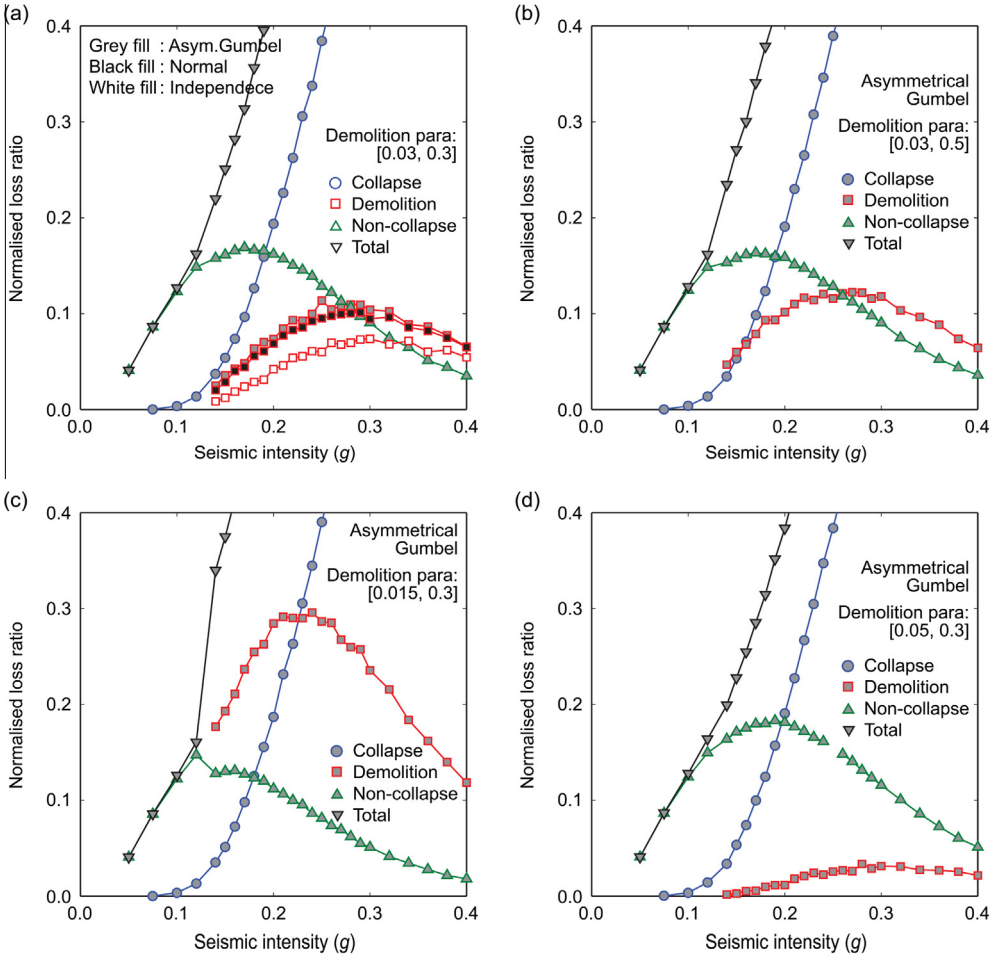

Fig. 15. Comparison of IM–DV functions for collapse, demolition, non-collapse damage, and total cost by considering different copula functions and demolition damage state limit parameters: (a) asymmetrical Gumbel, normal, and independence copulas with demolition parameters [0.03, 0.3], and (b) demolition parameters [0.03, 0.5], (c) demolition parameters [0.015, 0.3], and (d) demolition parameters [0.05, 0.3]. For (b–d), the asymmetrical Gumbel copula is employed.

curves for the asymmetrical Gumbel and the normal copulas are similar (as expected from Fig. 14), while that for the independence copula differs significantly from the other cases. For the independence copula, more failure cases occur as non-collapse loss, rather than demolition. This is the consequence due to the independent characteristics of MaxISDR and ResISDR and the avoidance of unrealistic ResISDR samples in simulation. This illustrates the importance of taking into account a realistic dependence structure of MaxISDR and ResISDR. The effects due to the adopted demolition limit state parameters are significant as illustrated in Fig. 15b–d. When the limit state function is more uncertain (Fig. 15b), the demolition loss increases by about 10–40%, depending on the IM level. When the median limit state for demolition is small (Fig. 15c), the demolition failure mode consists of about 30% of the entire failures (peaked at around IM equal to 0.22 g). On the other hand, when the median is large (Fig. 15d), the frequency of the demolition becomes small (less than 5%) and the collapse failure mode becomes dominant.

5. Conclusions

This study developed multi-variate seismic demand models using copulas, and applied them to a 4-storey non-ductile RC frame in Victoria, British Columbia, Canada. Key hysteretic characteristics of the non-ductile RC frame were captured in the finite-element model, which was capable of simulating damage initiation to collapse realistically. The method took into account multiple damage–loss generation modes due to non-collapse repairs, collapse, and demolition, which were evaluated in terms of inter-related EDP parameters, i.e. MaxISDR, ResISDR, and PFA. As the copula method captures upper tail and nonlinear dependence of key seismic demand variables and facilitates the separate modelling for marginal probability distributions and dependence functions, it is suitable for characterising EDP variables with heavy right tail whose marginal distributions cannot be represented by the normal or lognormal distribution (e.g. ResISDR). The seismic demand parameters were calculated based on IDA; thus the proposed method can be viewed as an extension to current IDA-based seismic demand estimation methods. Practically, the developed seismic demand models are useful for conducting detailed seismic loss estimation studies for a class of non-ductile RC buildings in Victoria, because up-to-date regional seismic hazard information and ground motion data were also incorporated as part of model development (e.g. multiple-CMS-based record selection and updated strong motion database that includes records from the 2011 Tohoku earthquake). The main results from the current investigations include that joint probabilistic modelling of MaxISDR, ResISDR, and PFA (at ground floor) was implemented successfully by adopting the Frechet/lognormal distribution for MaxISDR and PFA and the generalised Pareto distribution for ResISDR, while by adopting the asymmetrical Gumbel and normal copula functions for MaxISDR–ResISDR data pairs (note: PFA was modelled independently for the structural model). The effects of multi-variate seismic demand modelling on the

expected seismic loss ratios (i.e. mean IM–DV functions) were significant. The critical information is the demolition limit state curve (which was defined more or less arbitrarily in this study). In addition, the results indicated that consideration of a realistic dependence structure of MaxISDR and ResISDR can be important for seismic loss estimation as well as for multi-criteria seismic performance evaluation (where damage states are defined in terms of both MaxISDR and ResISDR).

Acknowledgements

Strong ground-motion data were obtained from the PEER-NGA database at http://peer.berkeley.edu/nga/, the K-NET at www.k-net.bosai.go.jp, the KiK-net at www.kik.bosai.go.jp, and SK-net (http://www.sknet.eri.u-tokyo.ac.jp/).

This work was supported by the Engineering and Physical Sciences Research Council (EP/M001067/1).

References

[1] Cornell CA, Krawinkler H. Progress and challenges in seismic performance assessment. PEER Center News 2000;3(2):1–4.
[2] Cornell CA, Jalayer F, Hamburger RO, Foutch DA. Probabilistic basis for 2000 SAC Federal Emergency Management Agency steel moment frame guidelines. J Struct Eng 2002;128(4):526–33.
[3] Goulet CA, Haselton CB, Mitrani-Reiser J, Beck JL, Deierlein GG, Porter KA, et al. Evaluation of the seismic performance of a code-conforming reinforced-concrete frame building – from seismic hazard to collapse safety and economic losses. Earthq Eng Struct Dyn 2007;36(13):1973–97.
[4] Jayaram N, Shome N, Rahnama M. Development of earthquake vulnerability functions for tall buildings. Earthq Eng Struct Dyn 2012;41(11):1495–514.
[5] Liel AB, Haselton CB, Deierlein GG, Baker JW. Incorporating modelling uncertainties in the assessment of seismic collapse risk of buildings. Struct Saf 2009;31(2):197–211.
[6] Liel AB, Haselton CB, Deierlein GG. Seismic collapse safety of reinforced concrete buildings. II: comparative assessment of non-ductile and ductile moment frames. J Struct Eng 2011;137(4):492–502.
[7] Vamvatsikos D, Fragiadakis M. Incremental dynamic analysis for estimating seismic performance sensitivity and uncertainty. Earthq Eng Struct Dyn 2010;39(2):141–63.
[8] Porter KA, Kiremidjian AS, LeGrue JS. Assembly-based vulnerability of buildings and its use in performance evaluation. Earthq Spectra 2001;17(2):291–321.
[9] Ramirez CM, Miranda E. Building-specific loss estimation methods & tools for simplified performance-based earthquake engineering. Technical Report No. 171, Stanford: John A Blume Earthquake Engineering Center; 2009.
[10] Kawashima K, MacRae GA, Hoshikuma J, Nagaya K. Residual displacement response spectrum. J Struct Eng 1998;124(5):523–30.
[11] Christopoulos C, Pampanin S, Priestley MJN. Performance-based seismic response of frame structures including residual deformations – part I: single-degree-of-freedom system. J Earthq Eng 2003;7(1):97–118.
[12] Ramirez CM, Miranda E. Significance of residual drifts in building earthquake loss estimation. Earthq Eng Struct Dyn 2012;41(11):1477–93.
[13] Vamvatsikos D, Cornell CA. Incremental dynamic analysis. Earthq Eng Struct Dyn 2002;31(3):491–514.
[14] Ruiz-García J, Miranda E. Residual displacement ratios for assessment of existing structures. Earthq Eng Struct Dyn 2006;35(3):315–36.
[15] Goda K. Statistical modeling of joint probability distribution using copula: application to peak and permanent displacement seismic demands. Struct Saf 2010;32(2):112–23.
[16] Uma SR, Pampanin S, Christopoulos C. Development of probabilistic framework for performance-based seismic assessment of structures considering residual deformations. J Earthq Eng 2010;14(7):1092–111.
[17] McNeil AJ, Frey R, Embrechts P. Quantitative risk management: concepts, techniques and tools. Princeton: Princeton University Press; 2005.
[18] Genest C, Favre AC. Everything you always wanted to know about copula modeling but were afraid to ask. J Hydrol Eng 2007;12(4):347–68.
[19] Uzumeri SM, Otani S, Collins MP. An overview of Canadian code requirements for earthquake resistant concrete buildings. Can J Civil Eng 1978;5(3):427–41.
[20] Ventura CE, Finn WDL, Onur T, Blanquera A, Rezai M. Regional seismic risk in British Columbia – classification of buildings and development of damage probability functions. Can J Civil Eng 2005;32(2):372–87.
[21] Hyndman RD, Rogers GC. Great earthquakes on Canada's west coast: a review. Can J Earth Sci 2010;47(5):801–20.
[22] Atkinson GM, Goda K. Effects of seismicity models and new ground motion prediction equations on seismic hazard assessment for four Canadian cities. Bull Seismol Soc Am 2011;101(1):176–89.
[23] Baker JW. The conditional mean spectrum: a tool for ground motion selection. J Struct Eng 2011;137(3):322–31.
[24] Goda K, Atkinson GM. Seismic performance of wood-frame houses in south-western British Columbia. Earthq Eng Struct Dyn 2011;40(8):903–24.
[25] Akaike H. A new look at the statistical model identification. IEEE Trans Automatic Control 1974;19(6):716–23.
[26] Luco N, Cornell CA. Structure-specific scalar intensity measures for near-source and ordinary earthquake ground motions. Earthq Spectra 2007;23(2):357–92.
[27] Liel AB, Deierlein GG. Assessing the collapse risk of California's existing reinforced concrete frame structures: metrics for seismic safety decisions. Technical Report No. 166, Stanford: John A Blume Earthquake Engineering Center; 2008.
[28] ICBO. Uniform building code. Pasadena: International Conference of Building Officials; 1967.
[29] Haselton CB, Liel AB, Lange ST, Deierlein GG. Beam-column element model calibrated for predicting flexural response leading to global collapse of RC frame buildings. Report 2007/03, Berkeley: Pacific Earthquake Engineering Research Center; 2008.
[30] Ibarra LF, Medina RA, Krawinkler H. Hysteretic models that incorporate strength and stiffness deterioration. Earthq Eng Struct Dyn 2005;34(12):1489–511.
[31] Luco N, Bazzurro P. Does amplitude scaling of ground motion records result in biased nonlinear structural drift responses? Earthq Eng Struct Dyn 2007;36(13):1813–35.
[32] Goda K, Taylor CA. Effects of aftershocks on peak ductility demand due to strong ground motion records from shallow crustal earthquakes. Earthq Eng Struct Dyn 2012;41(15):2311–30.
[33] Goda K. Nonlinear response potential of mainshock–aftershock sequences from Japanese earthquakes. Bull Seismol Soc Am 2012;102(5):2139–56.
[34] Tesfamariam S, Goda K. Loss estimation for non-ductile reinforced concrete building in Victoria, British Columbia, Canada: effects of mega-thrust M_w9-class subduction earthquakes and aftershocks. Earthq Eng Struct Dyn 2015. http://dx.doi.org/10.1002/eqe.2585.
[35] Touran MA, Suphot L. Rank correlations in simulating construction costs. J Constr Eng Manage 1997;123(3):297–301.
[36] BSSC. NEHRP recommended provisions for seismic regulations for new buildings and other structures. Washington: Building Seismic Safety Council; 2004.
[37] ATC. Seismic performance assessment of buildings: volume 1 – methodology (FEMA P-58-1). Redwood City: Applied Technology Council; 2012.